

Predicting Lifetime of Thick Al Wire Bonds Using Signals Obtained From Ultrasonic Generator

Elaheh Arjmand, Pearl A. Agyakwa, Martin R. Corfield, Jianfeng Li, and C. Mark Johnson, *Member, IEEE*

Abstract—Routine monitoring of the wire bonding process requires real-time evaluation and control of wire bond quality. In this paper, we present a nondestructive technique for detecting bond quality by the application of a semisupervised classification algorithm to process the signals obtained from an ultrasonic generator. Experimental tests verified that the classification method is capable of accurately predicting bond quality, indicated by bonded area measured by X-ray tomography. Samples classified during bonding were subjected to temperature cycling between $-55\text{ }^{\circ}\text{C}$ and $+125\text{ }^{\circ}\text{C}$, and the distribution of bond life amongst the different classes was analyzed. It is demonstrated that the as-bonded quality classification is closely correlated with thermal cycling life and can, therefore, be used as a nondestructive tool for monitoring bond quality and predicting useful service life.

Index Terms—Heavy wire bonding, power electronic, reliability, ultrasonic signal, X-ray tomography.

I. INTRODUCTION

IN POWER electronic modules, various components of different materials with different thermal expansion coefficients (CTE) are connected together. The main components are copper base plate, ceramic substrate, conductors, semiconductors, and wire bonds. The entire module is encapsulated with silicone gel, closed with a lid and finally screwed down onto a heat sink. For better thermal transfer from the module to the heat sink, a thin layer of thermal interface material is used (see Fig. 1). The manufacturing line of power electronic modules requires different assembly processes, such as soldering, ultrasonic wire bonding, direct diffusion bonding of copper, and pressure contacts.

Under operation conditions, power electronic modules dissipate heat. Differences in CTEs cause the materials expand and contract at different rates as the temperature fluctuates [1]. These thermomechanical load cycles can lead to degradation and failure of material in the interconnections and finally the whole module. For a high service life, therefore, the connections within the modules must be robust and reliable.

Manuscript received July 20, 2015; revised December 18, 2015; accepted February 23, 2016. This work was supported in part by the U.K. Engineering and Physical Sciences Research Council through the HubNet Project under Grant EP/I013636/1 and in part by Dynex Semiconductors Ltd., for providing the dies and DBC substrate tiles. Recommended for publication by Associate Editor J. J. Pan upon evaluation of reviewers' comments.

The authors are with the Electrical Engineering Department, The University of Nottingham, Nottingham NG7 2RD, U.K. (e-mail: eexea8@nottingham.ac.uk; pearl.agyakwa@nottingham.ac.uk; martin.corfield@nottingham.ac.uk; jianfeng.li@nottingham.ac.uk; mark.johnson@nottingham.ac.uk).

Color versions of one or more of the figures in this paper are available online at <http://ieeexplore.ieee.org>.

Digital Object Identifier 10.1109/TCPMT.2016.2543001

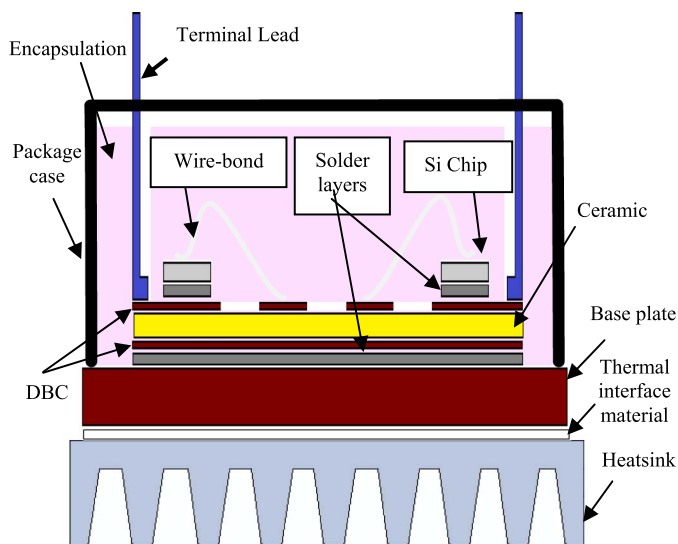


Fig. 1. Cross section view of power Insulated Gate Bipolar Transistor (IGBT) module package.

Therefore, it is important for power electronic packaging manufacturers to address the reliability issues at the design stage and on the manufacturing line [2].

Among the most lifetimes, limiting factors in power electronic module reliability are wire bond liftoff and bond heel cracking. Consequently, online evaluation of bond quality and early detection of defects have been a concern for many years. In general, the need for extracting reliable real-time information and analysis during the wire bonding process can be summarized as follows.

- 1) It can be used as a pretreatment method in the start-up of production, so that faults or abnormalities in the wire bonding process can be detected at the onset.
- 2) The production line can be optimized through online analysis. If the wire bonding system makes weak bonds continuously then the operator can detect the abnormality and stop the production.
- 3) Production processes can be streamlined by this methodology to identify varying bond quality to efficiently allocate modules to suitable applications.

II. EVALUATION OF BOND QUALITY

There are a number of issues with traditional wire bond quality evaluation methods, such as shear and pull tests. Apart from the fact that they involve the destruction of the bonds under evaluation and thus those bonds cannot be monitored

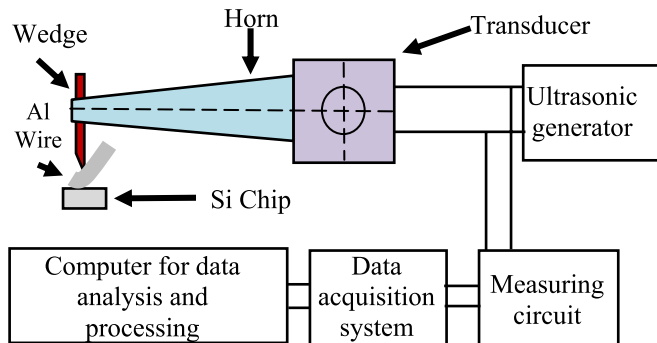


Fig. 2. Driving mechanism of ultrasonic wire bonder.

over their lifetime, they can also be more of an indication of the wire's mechanical properties, rather than the integrity of the interconnection itself. Unsurprisingly, there have been several efforts in the literature looking at ways of obtaining bond quality information without specimen sacrifice, with varying degrees of success. These include characterization of electrical impedance and output vibrations from the transducer [3]–[6]. Others have looked at the current envelope of the ultrasonic signals [3], [7]–[9]. Although a number of these methodologies are successfully able to discriminate between extremes of bond quality (i.e., good and bad bonds) [9], [10], none have demonstrated the ability to resolve subtle quality differences, as might occur within one production batch as a result of gradual tool wear, for example. More importantly, the influence of such slight changes in quality on the spread in predicted lifetimes has not been characterized.

In our previous work [11], we demonstrated a clear link between differences in bond quality arising from the changes in wire bonding parameters and the characteristics of the current envelope of the ultrasonic signals obtained from the transducer. In this paper, we examine whether the above method can be used to discriminate subtle quality differences arising from bonds made from the same parameters (e.g., as on a typical manufacturing line). A machine-learning algorithm is employed, and 3-D X-ray tomography is used as a nondestructive tool to evaluate the initial bond quality and its through-life degradation.

III. PRINCIPLES OF SIGNAL DETECTION

In this paper, an F&K Delvotec semiautomatic wire bonder was used. This wire bonder operates at a signal frequency of approximately 58 kHz. It consists of an ultrasonic generator and a bond-head. The main constituents of the bond-head are a transducer (piezoelectric driver), which converts the ultrasonic signals into mechanical oscillation, a voice coil motor, the bond tool (wedge), a touch-down sensor, a wire guide, and a cutter (see Fig. 2).

The ultrasonic generator has a phase-locked loop (PLL) controller, and during bonding, the PLL tunes the frequency output to the resonant frequency of the mechanical constituents, namely, the transducer, tool, and sample. Because the generator operates in constant-voltage mode, so the current signal varies according to the mechanical impedance presented to the transducer. Both the electrical impedance

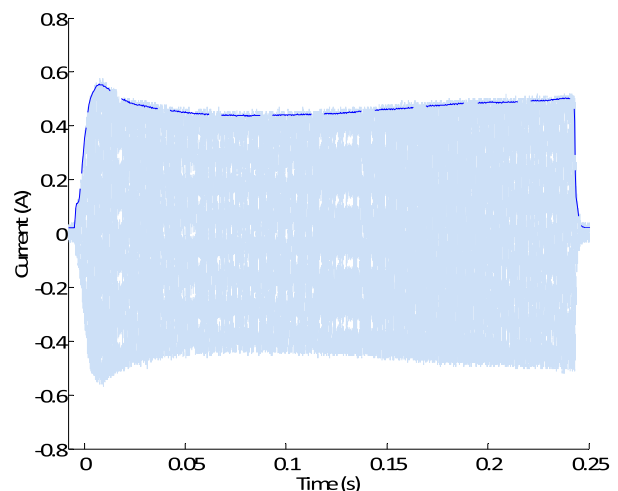


Fig. 3. Typical signature of bond signal and its corresponding envelope.

and the resonant frequency are influenced by the conditions at the bond interface during bonding. Thus, acquired current signals directly reflect bonding conditions. Fig. 2 also shows a schematic representation of the setup used in this paper for signal detection, acquisition, and analysis.

IV. FEATURE SELECTION AND CLASSIFICATION METHOD

Electrical signatures were recorded for each bond at a sampling rate of 12.5 MHz, in order to ensure that the signals collected could resolve the variations anticipated. The envelopes of the ultrasonic generator currents were computed using the MATLAB codes as follows. First, the bond signal was divided into 1000 intervals. Then, a fast Fourier transform (FFT) was performed for each interval, and the root mean square of the FFT magnitude was calculated at the frequency of interest for the corresponding interval. Fig. 3 shows a typical signature of a bonding signal and its corresponding envelope of current.

Our previous research confirmed that the current envelope of the electrical signal reflects the wire bonding machine parameters, and the correlation between the bond signal characteristics and the bond quality was confirmed by X-ray tomography images [11]. In this paper, this correlation between is examined for subtle change in bonding conditions, using a semisupervised learning algorithm. A semisupervised approach is appropriate in our case, because a small quantity of labeled data (imaged bonded area) is available, while unlabeled data are abundant. Semisupervised learning is halfway between supervised and unsupervised learning [12]. It is of practical value as it requires less training data than a fully supervised method and is preferable to an unsupervised approach in terms of accuracy [12]. Fig. 4 shows the typical procedures for a semisupervised algorithm.

Transductive support vector machine and cotraining are two of the well-known semisupervised algorithms [13]. Recently, researchers have shown an increased success with graph-based semisupervised learning algorithms as an initial guide for decision making [14]–[17]. In this paper, we used a semisupervised dimension reduction algorithm referred to

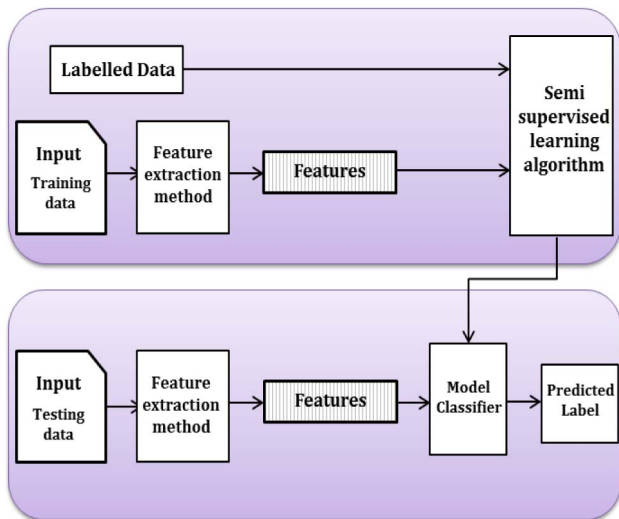


Fig. 4. Procedures for a semisupervised learning algorithm.

as semisupervised discriminate analysis (SDA) [13], [18] in order to classify bond signals with respect to their quality. It has been proposed that the SDA is able to reduce the dimensionality of data in semisupervised cases, achieving a much more efficient computation and has shown promising performance in a variety of applications [19].

SDA focuses on finding a projection which characterizes the discriminating structure from labeled data and also the inherent geometrical structure from both labeled and unlabeled data. In this algorithm, the labeled data points are specifically combined with unlabeled to build a graph incorporating neighborhood information. The graph allows a discrete approximation to the local geometry of the data manifold. Details of the workings of SDA algorithms are available in the literature [13], [18], [20].

V. EXPERIMENTAL PROCEDURE

A total of 513, 99.999% pure aluminum wires, $375\ \mu\text{m}$ in diameter, were ultrasonically bonded at room temperature onto silicon dies with a $5\text{-}\mu\text{m}$ -thick aluminum top metallization with the following bonding parameters: time: 250 ms; ultrasonic power: 145 digits; bond force start: 400 cN; bond force end: 900 cN; and touchdown steps: $100\ \mu\text{m}$. Bonding loop parameters were kept identical through all experiments (see Fig. 5).

The bond signals of the bonds on silicon dies (see Fig. 5) were collected at a sampling rate of 12.5 MHz. A Versa-XRM 500 machine supplied by Carl Zeiss X-ray microscopy was used for X-ray tomography. The bonds were subjected to passive thermal cycling from $-55\ ^\circ\text{C}$ to $+125\ ^\circ\text{C}$. From the 513 bonds, 24 bonds were randomly selected for X-ray tomography and imaged in their as-bonded condition, and then after 700 cycles and 1400 cycles. The remaining bonds were gently prodded with tweezers after every 100 cycles in order to record any liftoffs or failures.

VI. RESULTS AND DISCUSSION

The results of the 24 bonds randomly selected for X-ray tomography were analyzed by estimating the bonded area from

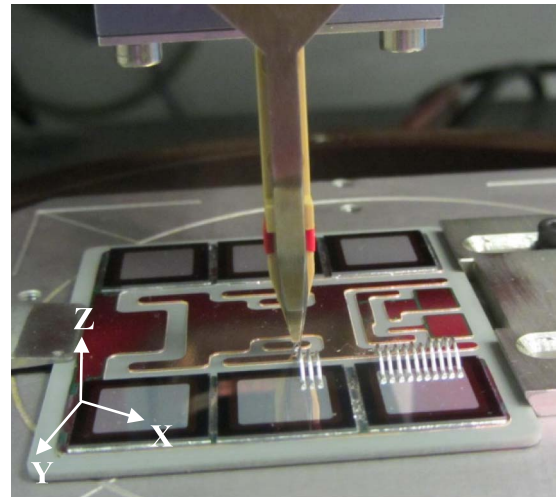


Fig. 5. Aluminum wire bonding on silicon dies.

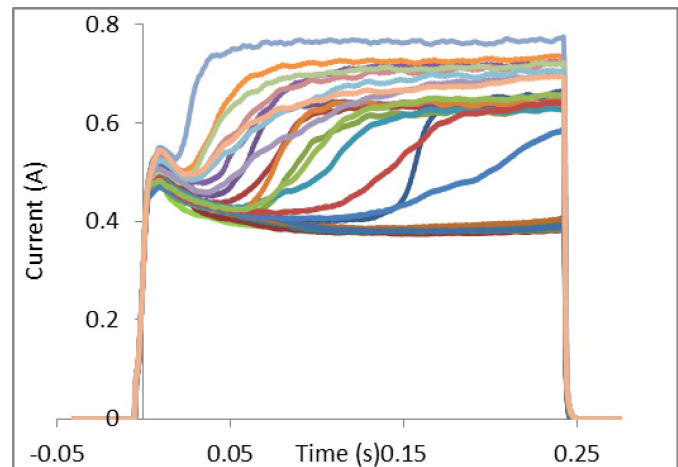


Fig. 6. Current envelope of 24 selected bonds.

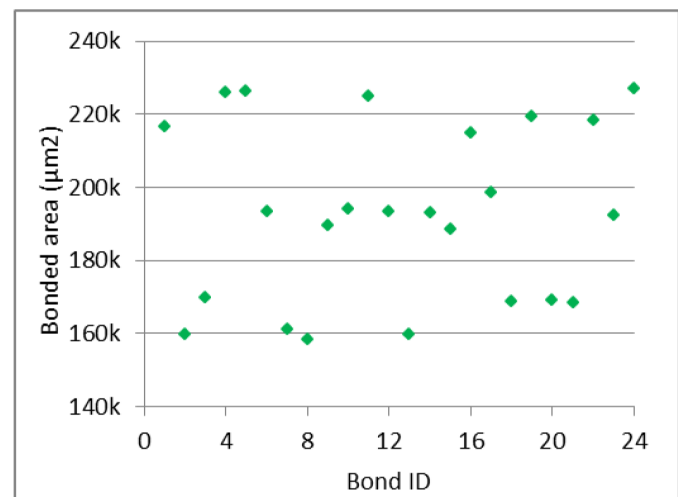


Fig. 7. Variation in bonded area in as-bonded condition.

2-D virtual cross sections of the interface in the xy plane. This was done using ImageJ, an open-source image processing and analysis software program. Figs. 6 and 7 show the variation in bond signal envelope and the bonded area of the selected wire bonds, respectively.

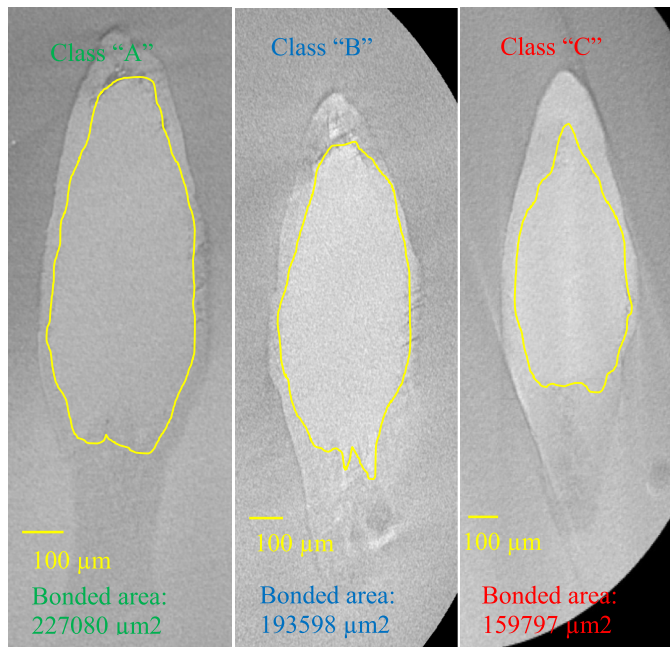


Fig. 8. X-ray tomography images of classified signals in the xy plane in as-bonded condition.

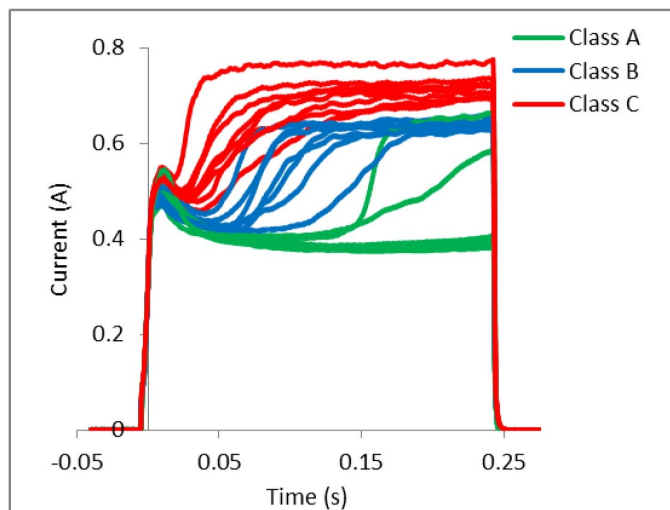


Fig. 9. Labeled signals according to measured bonded area.

According to the results of measured area, the bonds' signals were classified into three classes, A, B, and C, and the classified signals were used as labeled signals for the classification algorithm. The number of classes is usually arbitrarily chosen. In this case, we have been chosen three classes for simplicity; however, this can be any number greater than two. The bonds within class A had the largest attached area and those within class C had the least attached area. Fig. 8 shows the typical X-ray tomography images of the bonded area in each class. The labeled signals according to the measured bonded area are shown in Fig. 9. As can be seen, the bonds with largest attached area (class A) have a more uniform signal shape and received a more constant level of power compared with the bonds with the least attached area.

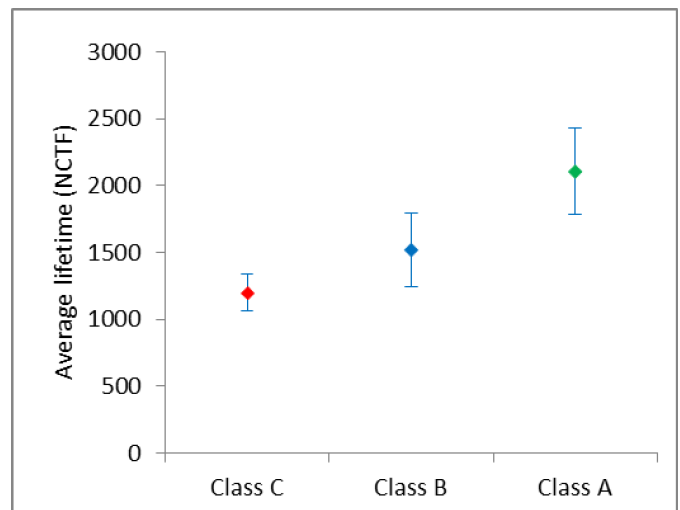


Fig. 10. Average lifetime of predicted classes.

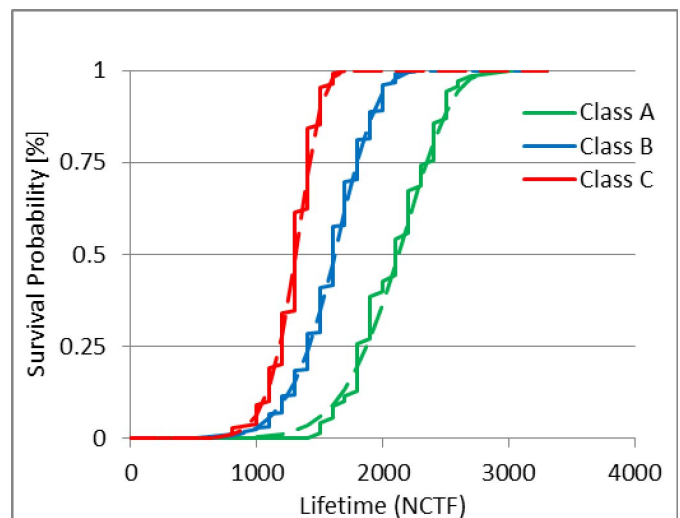


Fig. 11. Cumulative frequency curve of three classes.

A. Classification

The 20% of all bond signals, with the exception of those used as labeled data (98 bonds), were randomly selected as a training set, and the remaining bonds were selected for the test set (391 bonds). The SDA algorithm [13] was used to predict the bonds' classes. Meanwhile, all bonds were subjected to thermal cycling (-55°C to $+125^{\circ}\text{C}$) and inspected for the occurrence of liftoffs at 100 cycle intervals. Fig. 10 shows that the average lifetime of the class A bonds (with largest bonded area) is longer than either the class B or class C bonds. The results of model classifier performance thus indicate a strong correlation between the inferences of bond quality made from the bond signals and wire bond lifetime.

Cumulative frequency curves for the lifetime of the three classes are shown in Fig. 11. Clear separation of the lifetimes of the three classes can be observed, the onset of liftoff for class A bonds being almost a factor of 2 higher than for those in class C. The results of one-way analysis of variance (ANOVA) tests also confirm a significant

TABLE I
ONE-WAY ANOVA FOR WIRE BONDS LIFETIME DATA

Source	SS	DF	MS	F	P-value
Class	27862909	2	13931454	198.24	0.000
Error	27566861	388	702775		
Total	55129770	390			
S = 265.1 R-Sq =50.54% R-Sq(adj) =50.29%					

TABLE II
INDIVIDUAL 95% CONFIDENCE INTERVAL FOR THE
MEAN OF WIRE BOND'S LIFETIME DATA

Individual 95% CIs For Mean Based on Pooled StDev				
Level	Mean	StDev	-----+-----+-----+-----	
1	2100.0	320.3		(-*)
2	1594.8	283.5		(-*)
3	1291.7	172.7	(-*)	
-----+-----+-----+-----				
1250 1500 1750 2000				

TABLE III
PRECISION VALUE FOR EACH CLASS

Precision [%]		
Class "A"	Class "B"	Class "C"
91	69	83

difference in the lifetime of wire bonds among the three classes (see Tables I and II). This affirms the suitability of the method for monitoring the quality of the bonding process.

The overall accuracy of the classifier was assessed by comparing predicted classed and actual lifetime data. This is the sum of all correct classified bonds over total number of bonds. In this case, if we assume that the following holds.

- 1) Class A > 1800 cycles.
- 2) 1400 cycles ≤ class B ≤ 1800 cycles.
- 3) Class C < 1400 cycles.

Then, the overall accuracy would be 78%. The value of the overall accuracy obviously depends on the assumption made with regard to the lifetime boundaries of each class.

In addition to the overall accuracy, as described above, we can also describe our model in terms of two other performance indices: 1) precision values for individual classes derived as the number of correctly predicted bonds over the total number of predicted bonds in that class (see Table III) and 2) recall values for individual classes derived as the total number of correctly predicted bonds over the total number of actual bonds in each class (see Table IV).

B. Degradation Rate

The bonds randomly selected for X-ray tomography were imaged at 0 cycles (in the as-bonded condition), 700 cycles, and 1400 cycles. The reduction of attached area was measured to obtain the rate of degradation for the different classes. The results are given for both class C and class A. As can be

TABLE IV
RECALL VALUE FOR EACH CLASS

Recall [%]		
Class "A"	Class "B"	Class "C"
72	84	74

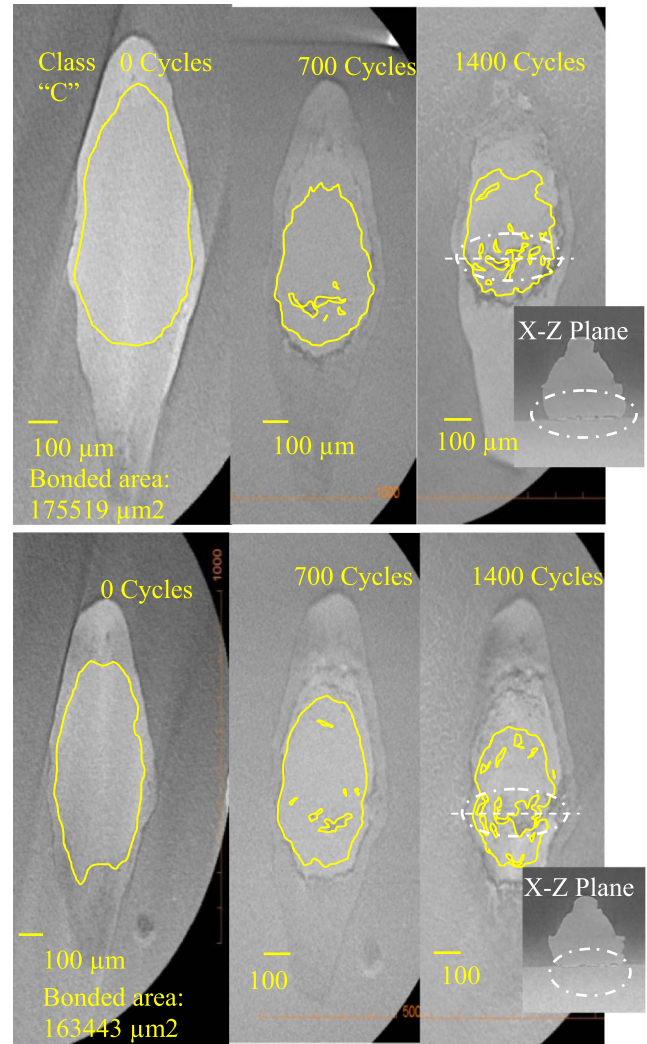


Fig. 12. X-ray tomography images of two bonds in class C in the xy plane in as-bonded condition, 700 cycles and 1400 cycles.

seen in Fig. 12, in the as-bonded condition, the bonds attached from the middle and significant precracks appear around the edge and in particular at the toe and heel of the bonds. After 700 cycles, cracks have started to grow inward from the edge, and microvoids have begun to coalesce. After 1400 cycles, the bond has almost lifted off as illustrated in the xz plane image inset in Fig. 12.

Fig. 13 shows that in the as-bonded state, the bonds in class A have a more bonded area compared with those in class C. Again, precracks are evident around the edge of the bond and in particular at the heel and the toe. After 1400 cycles, microvoids have started to join together. The rate of degradation, measured in terms of the remaining bonded area, for both

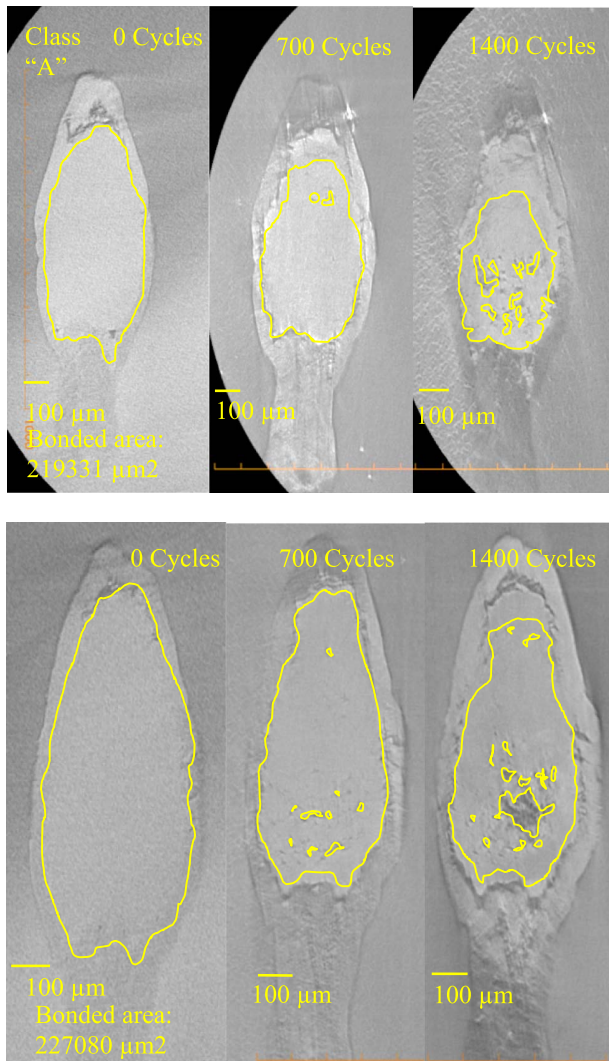


Fig. 13. X-ray tomography images of two bonds in class A in the *xy* plane in as-bonded condition, 700 cycles and 1400 cycles.

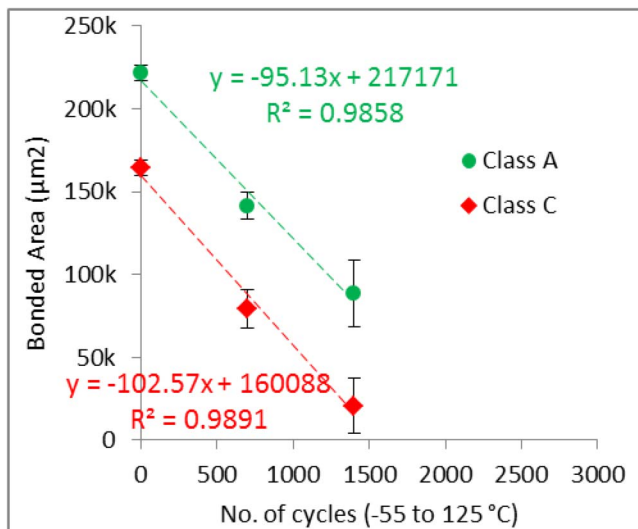


Fig. 14. Bonds degradation rate in classes A and C.

classes is shown Fig. 14. The results indicate that both classes degrade at almost the same rate, although the initial bonded area of the class A bonds is significantly higher, leading to

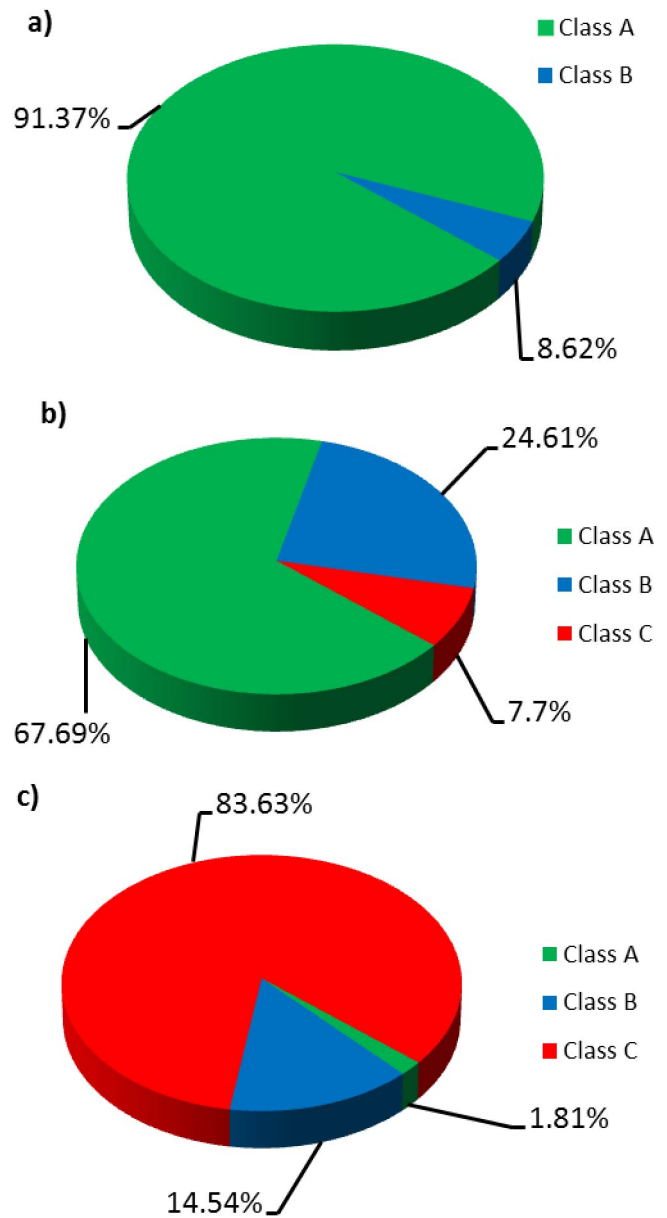


Fig. 15. Classification results in (a) using fresh and plasma-cleaned dies, (b) using fresh and without plasma cleaning, and (c) using old dies (stored for four days in purged cabinet) and without plasma cleaning.

longer life. The estimated lifetime from the linear regression lines in Fig. 14 agrees very well with the actual average lifetime of the predicted class of class A in Fig. 10. In class C, there is a slight difference between the estimated lifetime and the actual average lifetime. This might be because the bonds with a very small bonded area are prone to liftoff as a result of gentle prodding with the tweezers. Therefore, it might be a reason that the actual (tweezer test) lifetime is less than the lifetime estimated from the residual bonded area.

C. Surface Treatment

Evidence from the previous work obtained from the literature confirms that appropriate surface treatment prior to wire bonding improves wire-bonding strength by removing contamination. In this paper, we also checked the performance

of the presented method for different bond pad conditions. This is shown in Fig. 15, which shows the effect of bond surface condition on bond quality. In condition a, the bonds were made on freshly manufactured and plasma-cleaned dies, in condition b, bonds were made on freshly manufactured dies without prior plasma cleaning, and in condition c, bonds were made on manufactured dies which had been stored in a argon purged cabinet for four days at room temperature. The results from condition a shows that the samples contain no class C bonds, in other words no weak bonds, and also confirm the work of [21] that plasma cleaning can provide the best wire bonding quality. The results from condition c clearly illustrate how bond quality is reduced due to using old dies.

Overall, the method for bond quality assessment proposed in this paper has been shown to be capable of distinguishing between the differing levels of bond quality expected within a batch of bonds exhibiting typical variation, which are not solely due to the wire bonding machine and its parameters, but also due to other factors, including the condition of bond surface, such as cleanliness of die surface, freshness of die, and bonding environment condition.

In Fig. 10, the predicted classes of bond quality show some variation (see error bars), especially in bonds classified as class A. However, the classification is strong enough to demonstrate that the bonds may be separated into different quality groups for the purposes of online quality monitoring and evaluation of the wire bonding process. In addition, it is important to note that the accuracy of prediction of the model classifier can be improved by adding more labeled signals and increasing the size of the training set.

VII. CONCLUSION

In this paper, we have reported a nondestructive, online technique for detecting the quality of ultrasonically bonded wires by the application of a semisupervised classification algorithm to process signals obtained from the ultrasonic generator. The role of the semisupervised algorithm was to find the best model classifier using the labeled data and a training set.

The method is unique in providing a nondestructive way of evaluating wire bond quality in real time. All the steps followed in this paper, such as the signal acquisition, data analysis, classification, and lifetime production, can be carried out instantaneously on the production line with minimal additional infrastructural requirements. Therefore, it can be used to detect any fault or abnormality continuously and in real time, instead of relying on quality measurements at the end of a batch or at given sampling intervals. The choice of bonded area as the discriminating parameter at the time of bonding has the further advantage that it is correlated with thermal cycling lifetime and is, therefore, a good indicator of the in-service reliability of the bond. This can be applied to streamline production processes by, for example, grading predicted product life based on the proportion of high-quality bonds. The method can also be applied in the development of improved bonding processes, or as illustrated here, in the identification of optimized handling and cleaning methods.

Finally, the proposed method possesses significant improvement and effectiveness compared with other existing methods of real-time bond quality monitoring. In future work, it would be interesting to evaluate the accuracy of the model performance on new data sets, as it is important to have high performance with new data.

REFERENCES

- [1] H. Lu and C. Bailey, "Lifetime prediction of an IGBT power electronics module under cyclic temperature loading conditions," in *Proc. Int. Conf. Electron. Packag. Technol. High Density Packag. (ICEPT-HDP)*, Aug. 2009, pp. 274–279.
- [2] C. Bailey, H. H. Lu, C. Yin, and S. Ridout, "Predictive reliability, prognostics and risk assessment for power modules," in *Proc. 5th Int. Conf. Integr. Power Syst. (CIPS)*, Mar. 2008, pp. 1–7.
- [3] S. W. Or, H. L. W. Chan, V. C. Lo, and C. W. Yuen, "Sensors for automatic process control of wire bonding," in *Proc. 10th IEEE Int. Symp. Appl. Ferroelectr. (ISAF)*, vol. 2, Aug. 1996, pp. 991–994.
- [4] W. Feng, Q. Meng, Y. Xie, and Q. Meng, "Online quality evaluation of ultrasonic wire bonding using input electrical signal of piezoelectric transducer," in *Proc. WRI World Congr. Comput. Sci. Inf. Eng.*, Mar./Apr. 2009, pp. 462–466.
- [5] Z. W. Zhong and K. S. Goh, "Investigation of ultrasonic vibrations of wire-bonding capillaries," *Microelectron. J.*, vol. 37, no. 2, pp. 107–113, Feb. 2006.
- [6] H. Gaul, M. Schneider-Ramelow, K. D. Lang, and H. Reichl, "Predicting the shear strength of a wire bond using laser vibration measurements," in *Proc. 1st Electron. Systemintegr. Technol. Conf.*, Sep. 2006, pp. 719–725.
- [7] O. E. Gibson, W. J. Gleeson, L. D. Burkholder, and B. K. Benton, "Bond signature analyzer," U.S. Patent 4998 664, Dec. 22, 1989.
- [8] R. Pufall, "Automatic process control of wire bonding," in *Proc. 43rd Electron. Compon. Technol. Conf.*, Jun. 1993, pp. 159–162.
- [9] W. Feng, Q. Meng, Y. Xie, and H. Fan, "Wire bonding quality monitoring via refining process of electrical signal from ultrasonic generator," *Mech. Syst. Signal Process.*, vol. 25, no. 3, pp. 884–900, Apr. 2011.
- [10] E. Arjmand, P. Agyakwa, and C. M. Johnson, "Methodology for identifying wire bond process quality variation using ultrasonic current frequency spectrum," in *Proc. 15th Eur. Conf. Power Electron. Appl. (EPE)*, Sep. 2013, pp. 1–8.
- [11] E. Arjmand, P. A. Agyakwa, and C. M. Johnson, "Reliability of thick Al wire: A study of the effects of wire bonding parameters on thermal cycling degradation rate using non-destructive methods," *Microelectron. Rel.*, vol. 54, nos. 9–10, pp. 2006–2012, Sep./Oct. 2014.
- [12] X. Zhu and A. B. Goldberg, *Introduction to Semi-Supervised Learning*, R. Brachman and T. Dieterich, Eds. San Rafael, CA, USA: Morgan and Claypool Publishers, 2009.
- [13] D. Cai, X. He, and J. Han, "Semi-supervised discriminant analysis," in *Proc. IEEE 11th Int. Conf. Comput. Vis. (ICCV)*, Oct. 2007, pp. 1–7.
- [14] M. Belkin, P. Niyogi, and V. Sindhwani, "Manifold regularization: A geometric framework for learning from labeled and unlabeled examples," *J. Mach. Learn. Res.*, vol. 7, pp. 2399–2434, Nov. 2006.
- [15] J. Weston, C. Leslie, E. Ie, D. Zhou, A. Elisseeff, and W. S. Noble, "Semi-supervised protein classification using cluster kernels," *Bioinformatics*, vol. 21, no. 15, pp. 3241–3247, Aug. 2005.
- [16] T. Zhang and R. Ando, "Analysis of spectral kernel design based semi-supervised learning," in *Proc. Adv. Neural Inf. Process. Syst.*, vol. 18, 2006, p. 1601.
- [17] X. Zhu, Z. Ghahramani, and J. Lafferty, "Semi-supervised learning using Gaussian fields and harmonic functions," in *Proc. ICML*, 2003, pp. 912–919.
- [18] D. Cai, X. He, and J. Han, "SRDA: An efficient algorithm for large-scale discriminant analysis," *IEEE Trans. Knowl. Data Eng.*, vol. 20, no. 1, pp. 1–12, Jan. 2008.
- [19] J. Gui, Z. Sun, J. Cheng, S. Ji, and X. Wu, "How to estimate the regularization parameter for spectral regression discriminant analysis and its kernel version?" *IEEE Trans. Circuits Syst. Video Technol.*, vol. 24, no. 2, pp. 211–223, Feb. 2014.
- [20] D. Cai, "Spectral regression: A regression for efficient regularized subspace learning," Ph.D. dissertation, Dept. Comput. Sci., Univ. Illinois Urbana–Champaign, Champaign, IL, USA, 2009.
- [21] J. M. Nowful, S. C. Lok, and S.-W. R. Lee, "Effects of plasma cleaning on the reliability of wire bonding," in *Proc. Adv. Electron. Mater. Packag. (EMAP)*, Nov. 2001, pp. 39–43.



Elaheh Arjmand received the Degree in chemical industries from Tehran Technical College, Tehran, Iran, in 2006, and the M.Sc. degree in industrial quality technology from Newcastle University, Newcastle upon Tyne, U.K., in 2010. She is currently pursuing the Ph.D. degree with the Department of Electrical and Electronic Engineering, The University of Nottingham, Nottingham, U.K.

Her current research interests include characterizing wire bond process quality variation and its influence on uncertainty of physics of failure lifetime

predictions.



Pearl A. Agyakwa received the Degree in materials science from Brunel University, Uxbridge, U.K., in 1999, and the Ph.D. degree in metallurgy from The University of Nottingham, Nottingham, U.K., in 2004.

She has held a number of university positions since then, including one at the Advanced Manufacturing Research Centre, Boeing, Sheffield, U.K. She is currently a Research Fellow with the Department of Electrical and Electronic Engineering, The University of Nottingham, within a multidisciplinary team

of researchers studying various elements of power electronics packaging. Her current research interests include materials science aspects of interconnect reliability.

Martin R. Corfield received the B.Sc. degree in engineering science from the University of Hull, Kingston upon Hull, U.K., in 1996, and the M.Phil. and Ph.D. degrees in metallurgy and materials from the University of Birmingham, Birmingham, U.K., in 1998 and 2003, respectively.

He has held research fellowship positions with the University of Birmingham and The University of Sheffield, Sheffield, U.K. He is currently a Research Fellow with the Department of Electrical and Electronic Engineering, The University of Nottingham, Nottingham, U.K.



Jianfeng Li received the B.S. degree in mineralogy from Nanjing University, Nanjing, China, in 1991, and the M.S. and Ph.D. degrees in materials science from the Shanghai Institute of Ceramics, Chinese Academy of Sciences, Shanghai, China, in 1996 and 1999, respectively.

He was involved in thermal spray, laser materials processing, and high-temperature electronics with the University of Technology of Belfort, Montbéliard, France, the University of Manchester, Manchester, U.K., and King's College London,

London, U.K., until 2007. He is currently a Senior Research Fellow in Electronic Packaging and Interconnects for Power Electronics with The University of Nottingham, Nottingham, U.K.



C. Mark Johnson (M'90) received the B.A. degree in engineering and the Ph.D. degree in electrical engineering from the University of Cambridge, Cambridge, U.K., in 1986 and 1991, respectively.

He managed the U.K. national programme on silicon carbide electronics from 1998 to 2001, and in 2000, he became a Reader of Power Electronics with the University of Newcastle, Newcastle upon Tyne, U.K. In 2003, he was appointed as a Rolls-Royce/RAEng Research Professor of Power Electronic Systems with The University of Sheffield, Sheffield, U.K., and in 2006, he was appointed as a Personal Chair with The University of Nottingham, Nottingham, U.K., where he leads research on power semiconductor devices, power device packaging, reliability, thermal management, power module technologies, and power electronic applications.

He is the Director of the U.K. Engineering and Physical Sciences Research Council's Centre for Power Electronics, which combines U.K.'s best academic talent to address the key research challenges underpinning power electronics.